MSc in Photonics

PHOTONICS**BCN**

Universitat Politècnica de Catalunya (UPC)
Universitat Autònoma de Barcelona (UAB)
Universitat de Barcelona (UB)
Institut de Ciències Fotòniques (ICFO)

http://www.photonicsbcn.eu

Master in Photonics

MASTER THESIS WORK

EMODIN DIFFUSION IN CANCEROUS LIVING CELLS STUDIED BY MEANS OF RAMAN SPECTROSCOPY ENHANCED BY PLASMON EFFECTS

Mónica Marro Sánchez

Supervised by Prof. Dmitri Petrov, (ICFO, ICREA)
Sponsored by Fundació CELLEX Barcelona

Presented on date 9th June 2009

Registered at

Escola Tècnica Superior d'Enginyeria de Telecomunicació de Barcelona

Emodin diffusion in cancerous living cells studied by means of Raman spectroscopy enhanced by plasmon effects.

Mónica Marro Sánchez
ICFO-Institut de Ciències Fotòniques, Mediterranean Technology Park, 08860 Castelldefels (Barcelona), Spain

E-mail: Monica.Marro@icfo.es

Abstract. Emodin (6-methyl-1,3,8-trihydroxyanthraquinone) is considered as a potential candidate for photodynamic therapy for the treatment of cancer. A success in using of the molecule depends among other factors on the knowledge how fast it penetrates through the cell membrane and then diffuses inside the cell. A spatial distribution of emodin inside cancerous cells is also an important factor. The aim of this study is to investigate the diffusion of emodin in cancerous cells by means of a non invasive and sensitive technique: Surface Enhanced Raman scattering which permits us to study the evolution of the small amount of emodin inside single living cells. The experimental results were compared with a theoretical model that simulated the Brownian diffusion of particles. From this comparison and comparing with previous results in fluorescence spectroscopy we have found that: for a long time, emodin is accumulated in the cytoplasm in a region close to the membrane. The result is discussed in terms of emodin being stored in cell organelles located in the cytoplasm.

Keywords: Surface Enhanced Raman scattering, Brownian diffusion, emodin, cell, silver probe.

1. Introduction

Emodin (figure 1) is a natural occurring anthraquinone present in plants (rhubarb and buckthorn) of common use in traditional medicine and has been shown to have a potent anti-tumor effect. Previous studies have confirmed that emodin is a natural anti-angiogenic compound [1, 2] and produces a phototoxic effect on tumor cells [1, 3, 4]. For this reason emodin is considered as a potential candidate for photodynamic therapy [5]. However there is little knowledge of how fast it penetrates through the cell membrane and then diffuses inside the cell and the spatial distribution of emodin inside cancerous cells, factors of strong importance for efficiently using emodin for cancer treatments.

The aim of the present study is to investigate the diffusion of emodin in cancerous cells by means of a non invasive and sensitive technique: Surface Enhance Raman scattering.

Previous studies have been carried out with fluorescence and liquid chromatography [6]. Our research is a complement and permits us to study the cell out of the region of absorption of the molecule. Furthermore, our experiment provides information about the dynamic behaviour of emodin in a specific region of the cell. In our study we present a new way for monitoring the drug diffusion into single living cells and we have extracted some new results that we report in the conclusions.

First, the characteristics of Raman spectroscopy and SERS will be revised, followed by an explanation of the experimental setup and the methodology. Next, the experimental results will

be discussed along with a program that simulates the brownian diffusion of particles with conditions similar to our experiment. Finally conclusion will be made comparing the results with the previous studies and with simulation and we will propose some new hypothesis of how emodin diffuses and distributes inside the cancerous cell.

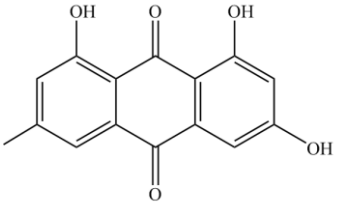

Figure 1. Chemical structure of emodin

1.1. Raman Spectroscopy

Raman spectroscopy is a technique where the vibrational and rotational levels of a sample can be studied. It is based on the observation of inelastic scattering (*Raman scattering*). In Raman spectroscopy, the sample can be irradiated by a laser beam from UV to IR region (ν_0), and the scattered light is analysed. The scattered light consists of two types: *Rayleigh scattering*, which is a elastic process and therefore the light has the same frequency as the incident beam (ν_0), and *Raman scattering* which is inelastic, considerably weaker (1 over 10^7 incident photons are Raman scattered photons) and has frequencies different than the incident light. Raman scattering can be of two types: *Stokes* line with frequency ν_0-ν_m and *anti-Stokes* line with ν_0+ν_m (figure 2). In Raman Spectroscopy, the peaks are measured as a shift with respect to the incident beam frequency (ν_0). It leads to a spectrum that is a fingerprint of the molecule used.

Raman scattering can be explained by classical theory. The incident light is described as a electromagnetic wave (laser beam) where the electric field strength associated fluctuates with time (t) as:

$$E = E_0 \cos 2\pi\nu_0 t \qquad (1.1)$$

where E_0 is the vibrational amplitude and ν_0 is the frequency of the incident light. The interaction of this incident light with a diatomic molecule results in an electric dipole moment P induced in the molecule:

$$P = \alpha E = \alpha E_0 \cos 2\pi\nu_0 t \qquad (1.2)$$

which is proportional to the electric field strength with a proportionality constant α called *polarizability*. If the molecule has a vibrational frequency ν_m, the nuclear displacement q can be described as:

$$q = q_0 \cos 2\pi\nu_m t \qquad (1.3)$$

where q_0 is the vibrational amplitude. In the case of small amplitude of vibration, α is a linear function of q:

$$\alpha = \alpha_0 + \left(\frac{\partial\alpha}{\partial q}\right)_0 q_0 + \cdots \qquad (1.4)$$

where, α_0 is the polarizability at the equilibrium position, and $\left(\frac{\partial\alpha}{\partial q}\right)_0$ is the rate of change of α with respect to the change in q, evaluated at the equilibrium position.

If we combine (1.2, 1.3 and 1.4), we obtain the dipole moment induced is:

$$P = \alpha E_0 \cos 2\pi\nu_0 t = \alpha_0 E_0 \cos 2\pi\nu_0 t + \left(\frac{\partial\alpha}{\partial q}\right)_0 q E_0 \cos 2\pi\nu_0 t =$$

$$= \alpha_0 E_0 \cos 2\pi\nu_0 t + \left(\frac{\partial\alpha}{\partial q}\right)_0 q_0 E_0 \cos 2\pi\nu_0 t \cos 2\pi\nu_m t = \qquad (1.5)$$

$$= \alpha_0 E_0 \cos 2\pi\nu_0 t + \frac{1}{2}\left(\frac{\partial\alpha}{\partial q}\right)_0 q_0 E_0 [\cos\{2\pi(\nu_0 + \nu_m)t\} + \cos\{2\pi(\nu_0 - \nu_m)t\}]$$

From this equation it can be seen three terms: the first term represents an oscillating dipole that radiates light of frequency ν_0 (Rayleigh scattering), the second term corresponds to the Raman scattering of frequency $\nu_0 + \nu_m$ (anti-Stokes) and the third term also represents Raman scattering with a frequency $\nu_0 - \nu_m$ (Stokes). From (1.5), if $\left(\frac{\partial\alpha}{\partial q}\right)_0$ is equal to zero, the vibration is not

Raman-active. Thus, the rate of change of polarizability (α) with the vibration must not to be zero for having a vibration Raman-active.

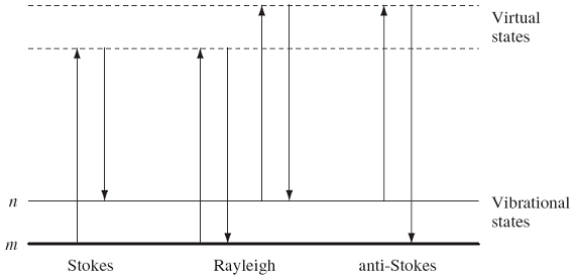

Figure 2. Comparison of energy levels for the Stokes, Rayleigh and anti-Stokes Raman spectra.

Figure 2 illustrates the different types of scattering in terms of the energy level in a molecule. In classical Raman spectroscopy, the energy of the excitation line is smaller than the first electronic excited state. The dotted line indicates a "virtual state" to distinguish it from the real excited state. According to Maxwell-Boltzmann distribution law, the probability to find a molecule in the ground state is larger than at excited vibrational states under normal conditions. Due to this, the Stokes (S) lines are stronger than the anti-Stokes (A) lines under normal conditions. As from both the same information can be obtained, normally only the Stokes side of the spectrum is measured because it gives stronger intensity.
Resonance Raman (RR) occurs when the exciting light wavelength is near to the maximum absorption region of the studied sample.

1.2. Surface Enhanced Raman Spectroscopy
Raman spectroscopy is a very useful technique in various research fields because provide us structural information of the sample used. However Raman signals are weak and therefore we are not able to investigate substances in low concentrations. One possible solution is surface-enhanced Raman scattering. Within a few years, strongly enhanced Raman signals were found for many different molecules, which had been attached to "SERS-active substrates" [8]. These SERS-active substrates are different types of metallic structures with sizes on the order of tens of nanometers: colloidal silver or gold particles in the 10- 150 nm size range, silver or gold electrodes or evaporated films of these metals. By means of SERS-active substrates Raman signal can be enhanced by a factor of $10^4 - 10^{15}$ [9], depending on the applied method. In order to enhance the signal of a molecule, it has to be adsorbed on metal surface or placed a few nanometres of distance (20-50 nm) to the SERS-active substrate. Due to this we are able to acquire signal from a very specific point of our sample.
The mechanism leading to the surface enhancement is not completely understood yet. In general there are two main contributions: the electromagnetic and the chemical charge transfer (CT) mechanism.

1.2.1 Electromagnetic enhancement. The electromagnetic contribution of the SERS enhancement is based on a plasmon excitation due to the incident laser light on the metal surface. This incident light excites the electrons in the metal which oscillate against the metal cores (called a surface plasmon). Having nanostructured surfaces, the oscillation of surface plasmon lead to an electromagnetic field, which reaches out of the metal surface, where the analyte is located. Therefore, in electromagnetic enhancement is not necessary to have attached the analyte. Due to the fact that the incident laser light has to excite the surface plasmon, it has to be adapted for the plasmon wavelength of each metal and the nanostructure of the metal surface. In order to accomplish this using the most common metals as SERS-active substrates (like silver and gold), SERS excitation lines cover mainly the visible spectral region up to the near infrared (NIR) between 450 and 1064 nm [10]. Excitation with UV light has also been reported [11].
1.2.2 Chemical enhancement. Experiments revealed that there was a second enhancement mechanism [20]. A resonance Raman mechanism can explain the observations and there are two

hypotesis (a) in the adsorbate the electronic states are shifted and broadened due to their interaction with the surface or (b) new electronic states are created because of the chemisorption and they serve as resonant intermediate states in Raman scattering. The results of experiments support the second hypothesis. Normally, the highest occupied molecular orbital (HOMO) and lowest unoccupied molecular orbital (LUMO) of the adsorbate are symmetrically placed in energy with respect to the Fermi level of the metal. With this configuration charge-transfer between the metal and the molecule can occur at about half the energy of the intrinsic difference in energy levels of the adsorbate. Due to this charge transfer, in chemical enhancement the analyte has to be in contact with the metal surface.

2. Experiment and methods

2.1. Experimental setup

Figure 3 represents the setup which consists of a 785 nm laser beam for Raman excitation with a power of about 5-7 mW at the sample. Firstly, laser light passes through a band pass filter and a beam expander and arrives to a notch filter. Notch filter has a cut-off frequency of 785nm and therefore transmission for this wavelength is zero. On the contrary the reflection is almost 100% for 785nm. From notch filter the light arrives to a 100x 1.3 numerical aperture oil immersion objective. The size of the focal spot was estimated to be 0.5 μm perpendicular to and 1 μm along the optical axis, i.e., less than the probe diameter. We use the backscattered geometry for collecting the Raman spectra. The backscattered light is collected by the objective and arrives to the dichroic mirror. There, a part of the light arrives to the CCD where we observe the real image from the microscope (figure 4). The rest of the light is reflected and passes through the Notch filter which finally removes the light with the same frequency than the excitation light. Our system has a confocal system formed by two lenses and one pinhole (150μm of diameter) that only allow passing light from the plane (confocal volume) [12] where the excitation laser is focused on the sample. Finally, the Raman scattered light is focused on the slit of the spectrometer (Acton Research, SpectraPro 2500i) and the Raman spectrum is recorded with a CCD camera with a spectral resolution of 3 cm^{-1}. In our case we use a grating of 600 lines/mm and blazed on 750 nm which means that at a wavelength 750 nm the efficiency is maximum (70%) and therefore we have almost all the energy concentrated at the zero order (for this wavelength) and less energy in higher orders.

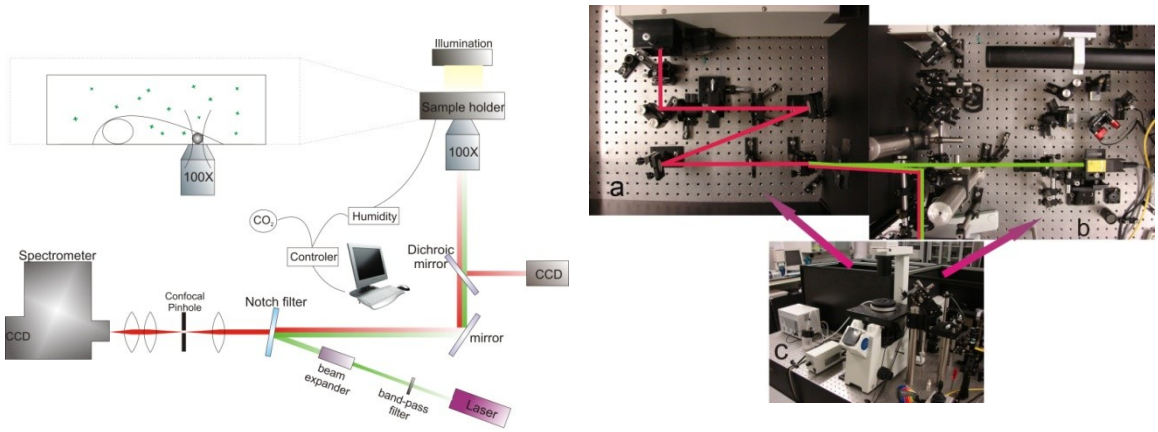

Figure 3. Experimental setup

The CCD of the spectrometer is cooled down to -100ºC and uses thermoelectric cooling. It uses the Peltier effect to create a heat flux between the junction of two different types of materials. A Peltier cooler, is a solid-state active heat pump which transfers heat from one side of the device to the other side against the temperature gradient, with consumption of electrical energy.
During the experiment the sample is incubated in the sample holder with following conditions: a temperature of 37°C and a controlled flux of 5% of CO_2 and 40% of humidity.

2.2. Sample preparation

Human glioma cells (U-87 MG line) were cultured as a monolayer and were grown in Dulbeccos modified Eagle medium (DMEM) containing L-glutamine (862 mg/L), sodium pyruvate (110 mg/L) and glucose (4500 mg/L), supplemented with 10 % fetal calf serum, penicillin (50 µg/mL) and streptomycin (50 µg/mL). Cells were maintained at 37 °C in a humidified 5 % CO_2 atmosphere. One day prior to experiments, cells were plated in plastic petri dishes (35 mm with a #0 thick cover glass on the bottom) at an optimal density of 4 x 10^5 cells/mL and incubated with 2 µm size silver covered silica bead during the night. During this time cells absorb beads and they are stored in the cytoplasm near to the membrane. In the experiments silver covered silica beads were used as probes because silver colloids on the surface acted as SERS-active substrates. This Silver covered metal beads were prepared by modification of the silica surface with APTMS ((3-aminopropyl)trimethoxysilane). Silver colloid nanosize particles were prepared by well known method described by Lee and Meisel [13]. Modified beads were mixed with metal nanoparticles to obtain a homogeneous coverage of metal on the bead [14].

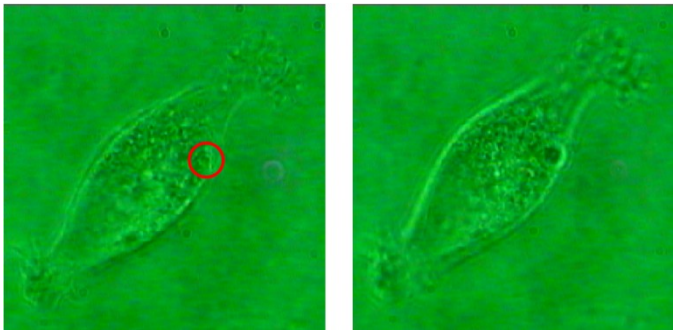

Figure 4. View of the cell with a bead inside. Left: the cell membrane of the cell is focused and we are not able to distinguish the bead. Right: Membrane is defocused and we can observe the bead.

2.3. Methodology

In order to measure the diffusion of emodin inside the cell we used 2 µm silica bead covered with silver colloids [14] as SERS-active substrate for detecting and measuring the Raman spectra of emodin. Those beads were absorbed by the cell and stored close to the membrane in the cytoplasm. This technique permitted us to detect the evolution in time of the amount of emodin in a specific region of the living cell. In order to obtain better and contrasted results we used two methods:

- The cells were pre-incubated during 4 hours with a fresh culture medium containing 2 µM concentration of emodin. After incubation the cells were rewashed three times in a culture medium. During experiments, the cells were enclosed in the sample holder and the excitation beam is focused onto a bead situated inside of the cell.
- While the sample was incubated in the sample holder, the excitation beam was focused onto a bead situated inside of the cell. Later, a drop of emodin (2 µM) was added in the solution of the cells. At this time, we start to detect the presence of emodin in the region of interest.

2.4. Data analysis

In the collected Raman spectra there are various types of noise. One of them is the background which is removed with a Mathematica software based on the established method [15]. In order to remove the spikes, select the desired peaks and plot the time dependence of the intensity of the emodin peaks we used Origin 7.

2.5 Simulation

In a theoretical model we have modified a program from F.Salvat (Universitat de Barcelona, Facultat de Física, *Estructura i constituents de la matèria*) that simulates the Brownian motion

of particles. We modified this software obtaining the diffusion of particles in a specific region (detection region) of a volume (cell and external media) and changing the conditions of the cell environment: temperature, diffusion coefficient and initial concentration of particles.

2.5.1. Brownian diffusion simulation

In this software we simulate numerically the Brownian diffusion; it means the particles that suffer thermal fluctuations and friction. The most general equation to describe this type of movement is the Langevin equation,

$$m\frac{\mathrm{d}\mathbf{v}}{\mathrm{d}t} = -\lambda\mathbf{v} + \vec{\chi}(t) \qquad (2.1)$$

where *m* is the mass of the particle, **v** his velocity and $\vec{\chi}(t)$ is the thermal noise. This last term is a random gaussian process. Here, we have considered the limit of high friction, in which the Langevin equation is reduced to:

$$\frac{\mathrm{d}\mathbf{r}}{\mathrm{d}t} = \vec{\eta}(t), \qquad (2.2)$$

where $\vec{\eta}(t) = \vec{\chi}(t)/\lambda$ is a random gaussian process with zero average and correlation

$$\langle \eta_i(t)\eta_j(t')\rangle = \frac{2k_BT}{\lambda}\delta_{ij}\delta(t-t') \qquad (2.3)$$

being η_i the cartesian components of $\vec{\eta}$. The variance of each component $\eta_i(t)$ is

$$\mathrm{var}\,\eta_i(t) = \int\langle \eta_i(t)\eta_j(t')\rangle \mathrm{d}t' = \frac{2k_BT}{\lambda} \qquad (2.4)$$

The program simulates the equation 2.2 with a gaussian noise that has the property 2.3. In order to be able to visualize the results, we consider the movement in a plane. It can be prove that if we analyze the random trajectories of a high collectivity of particles:

- The mean value of the position remain constant
- The movement is diffusive, with a diffusion coefficient **D** whose components are:

$$D_i \equiv \lim_{t\to\infty}\frac{\langle {r_i}^2(t)\rangle - \langle r_i(t)\rangle^2}{2t} = \frac{k_BT}{\lambda}$$

This is the Einstein's relation, $D_x = D_y = \frac{k_BT}{\lambda}$.

The simulation algorithm is the following. We consider NP independent particles that depart the origin at the instant t=0 and their movement follow the equations 2.2 and 2.3. We calculate the evolution by measuring their displacement during small time steps Δt. In each step, the coordinates of the particle *n* are modified in accordance with:

$$x_n(t+\Delta t) = x_n(t) + \Delta x$$
$$y_n(t+\Delta t) = y_n(t) + \Delta y$$

where the components Δx and Δy of the displacement are random gaussian numbers with zero average and variance equal to $\Delta t\frac{2k_BT}{\lambda}$.

2. Results

3.1. Experimental results

First of all, in order to identify and know the characteristic and better peaks for emodin in the samples, we obtained separately the Raman spectra of emodin $2\cdot10^{-6}$ M and the Raman spectra of cell, both with a metal covered bead in the confocal volume of the spectrometer (figure 5). From the graphs it can be observed that for 1170cm^{-1} and for 1334cm^{-1} Raman spectrum of emodin has peaks [16] as well as that the Raman spectrum of cell does not have peaks in this region. For this reason we have chosen these two peaks in order to analyze the behaviour of the quantity of emodin in the detection volume over time.

Finally, by following the procedures reported in the methodology, we obtained the graphs of figure 6. The two methodologies that have been used permit us contrast the results. With the first method a considerable amount of data can be obtained because it is possible to make an average of various cells in one single experiment. However, experiments have to be carried out in a very short time due to the fact that emodin can diffuse out of the cell because we wash the sample and put new media without the presence of emodin.

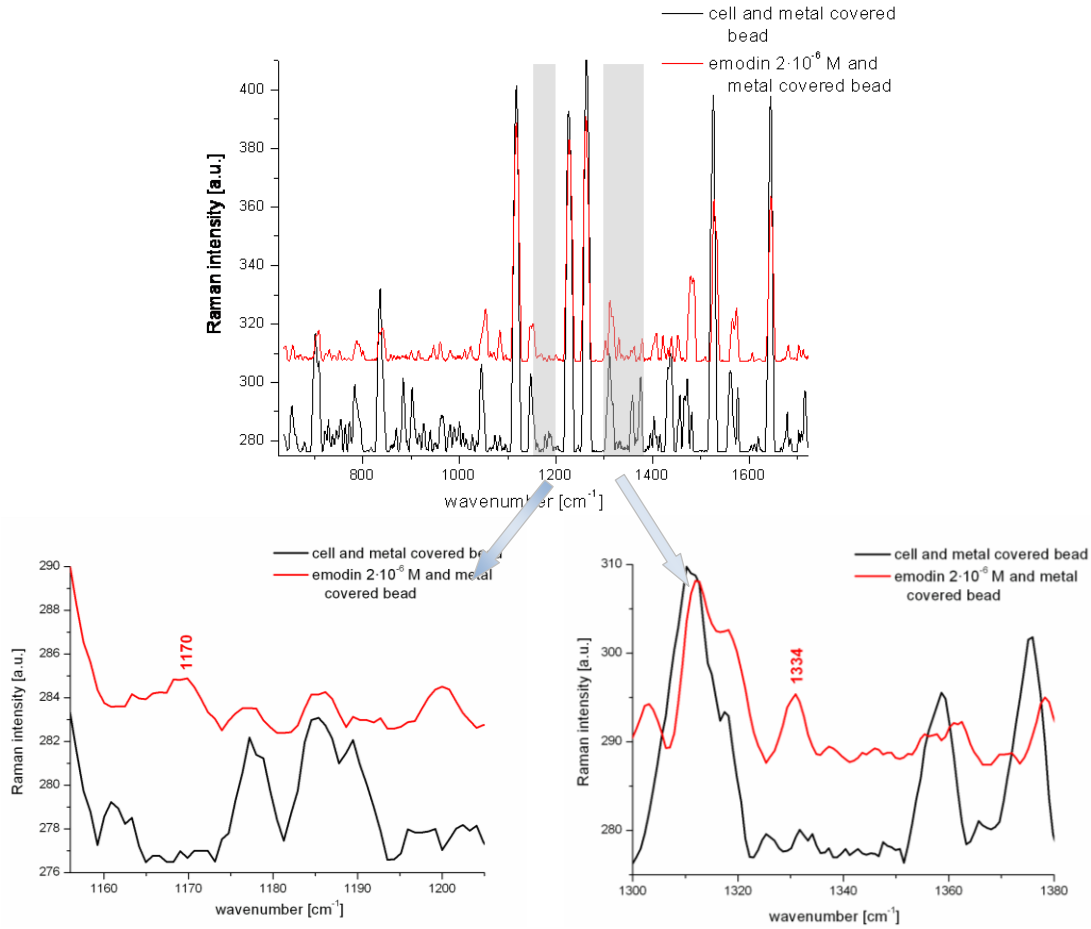

Figure 5. Raman spectrum of emodin ($2 \cdot 10^{-6}$ M) (red line) and cell (black line) both measured in the presence of a metal covered bead.

The second method describes the natural diffusion in a way more close to the reality and permits us to observe the behaviour of the Raman intensity in each minute. However it is not possible to do an average of various cells in the same experiment because the Raman excitation is carried out only in one single cell in each experiment. Therefore we obtain more temporal resolution but we have to perform more experiments and samples in order to have statistically significant results.

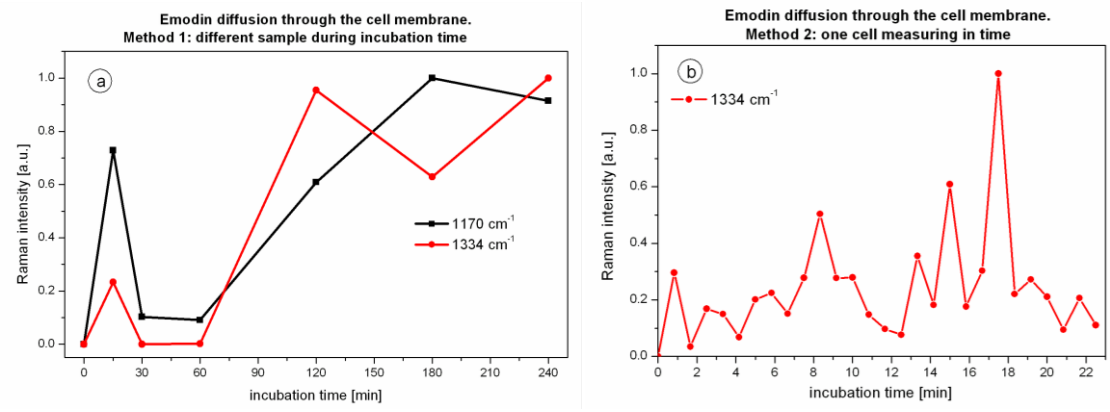

Figure 6. Distribution of main Raman bands of emodin inside cell over incubation time following the first (a) and the second (b) method.

3.2. Simulation results

In order to simulate as real situation with conditions similar to our problems, we defined a cell with 100 μm in size and the parameters of the configuration were:

- $D = 6000\mu m^2/min$ due to the fact that this is a common value for biomolecules like emodin diffusing in a liquid similar to water and with a temperature around 37^0C. Therefore: $\lambda = \frac{k_B T}{D} = 2.57 \cdot 10^{-6} g/min$ (with T=37^0C).
- 10^5 particles
- Membrane situated at 500 μm of the origin where the drop of particles starts to move and a region of detection of 1 μm of width.
- 2200 screenshots that corresponds to 308 minutes.

The program simulates that at the initial time all the molecules are in the origin of coordinates. The region to be studied that represent the zone where the bead can detect the presence of emodin is situated at 500 μm of the origin and is 1 μm of width. We also simulated that the particles could not escape out of a volume of 3x3 cm. However, more sophisticated conditions could be imposed. From figure 7 it can be seen the results of this simulation.

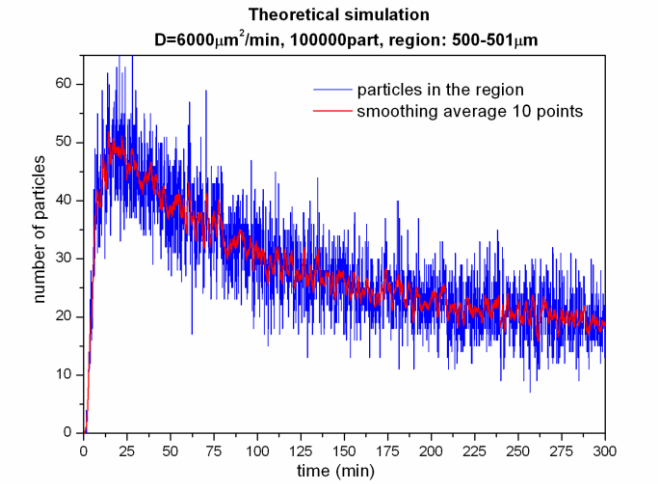

Figure 7. Theoretical simulation of diffusion of particles through the defined volume

Other simulations with the same code were carried out in order to probe the different behaviour for different temperatures (different diffusion coefficients *D*). It can be seen from the graphs below (figure 8) that the higher the diffusion coefficient is, the more rapid the diffusion of particles is.

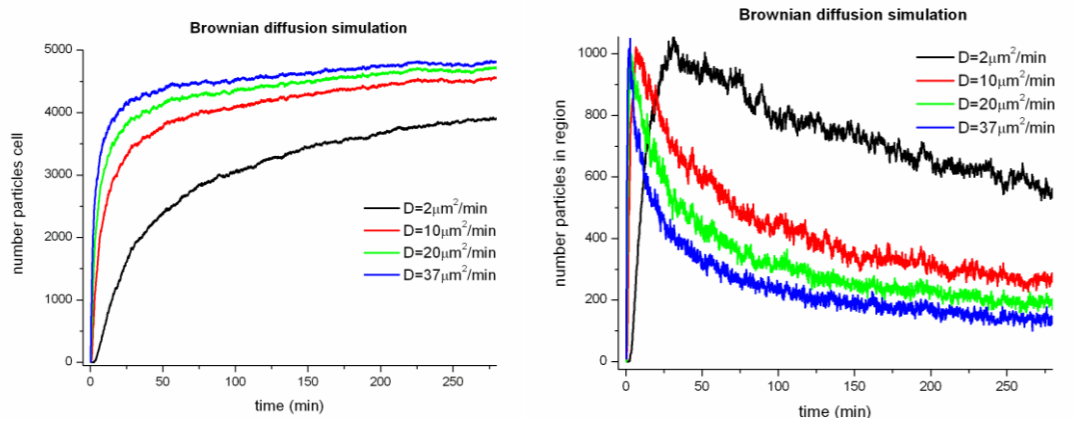

Figure 8. Different behaviour for different diffusion coefficients. The studied region was situated at 10 μm of the origin with 5 μm of width. Left: number of particles that pass the studied region over time. Right: number of particles that we obtain in the region of study over time.

4. Discussion

As can be seen in the experimental graphs (figure 6), there are three different stages. In the first 15 minutes the amount of the detected emodin increases until it reaches a maximum. In the second part (up to 60 minutes) the amount of emodin decreases and in the third stage it starts growing up to reach saturation (figure 6a).

In the first stage of the experiment the molecules start to dissolve in the membrane because they are lipophilic and the probe can detect them because beads are situated close to the membrane in the cytoplasm. In the next stage molecules diffuse throw the membrane and start to diffuse inside the cytoplasm. Due to this fact we observe a decrease in the amount of detected particles because the concentration of particles in the region of detection starts to decrease.

In contrast, from the simulated graphs it can be seen that we only have a peak at 15 minutes and then the amount of detected particles decreases up to reach saturation.

In the first part of simulated (figure 7) and experimental graphs (figure 6) molecules arrive to the membrane and our region of detection. For this reason we observe in both graphs an increase in the detected amount of emodin. Then the particles start to diffuse inside the cell and consequently the number of particles decreases. Up to here both experimental and simulated graphs coincide. However in the third stage we observe an increase of molecules in experimental plots. In principle, we would not expect this result because if molecules diffuse to the entire cell we would have to arrive to a stable situation in which the concentration of molecules in the region of detection would be constant. This change in experimental graphs may be due to the fact that molecules accumulate in the cytoplasm in some organelles close to our bead (mitochondria, ribosome...). Our experimental plots do not take into account this accumulation and the pathway that emodin follows inside the cell. Therefore they do not show this behaviour.

Thus, it can be concluded that emodin diffuse like simple diffusion [14, 15] in human glioma cells and it could be accumulated (stored) in some organelles in the cytoplasm close to membrane.

There are previous studies of the diffusion of this molecule in cancerous cells in fluorescence or HPLC [6]. However the behaviour that they observed is simple diffusion (taking into account the entire cell). This may be due to the fact that in organelles emodine is concentrated in big amounts that make it aggregates. When emodin is aggregated it changes chemical properties and therefore fluorescence could not be able to detect it. On the contrary, by Raman spectroscopy we are observing the vibrations of molecules; therefore also aggregates can be detected.

5. Conclusion

During the last years, Emodin, an anthraquinone molecule, has been proposed as a potential strong candidate for the photodynamic therapy by the treatment of some type of cancer [3]. A success in using of emodin depends among other factors on the knowledge how fast it penetrates through the cell membrane and then diffuses inside the cell. This work presented a new way for drug diffusing monitoring. SERS was used to detect the amount of emodin inside single living cells.

From the experimental and simulated results it can be concluded that emodin diffuse like simple diffusion in Human glioma cells and it could be accumulated (stored) in some organelles in the cytoplasm close to membrane.

Previous studies of the diffusion of this molecule in cancerous cells [6] showed that it is simple diffusion more close to simulated results. In contrast, we observed a different behaviour for long incubation times (the Raman intensity increases up to reach saturation).This may be due to the fact that in organelles emodin is concentrated in big amounts that aggregate. The aggregation of emodin can change his chemical properties and therefore fluorescence could not be able to detect it.

In conclusion we may say that SERS can be also used for monitoring of drug diffusion with higher sensitivity than fluorescence and it permit us to detect lower concentrations of molecules in very specific and small region in single living cells.

Acknowledgments
This research was funded by the Fundació Cellex Barcelona. I am indebted to my tutor and co-tutor Prof. Dmitri Petrov and Stefan Balint for their help and encouragement throughout the course of this work. I also want to thank Satish Rao, Prof. Francesc Salvat (UB), Jose M. Sancho (UB) and the rest of the members of my group at ICFO for their helpful conversations and comments. This work could not be carried out without the collaboration with Prof. Joan Seoane (Hospital Vall d'Hebron) who provided us the cells.

References

[1] Vargas F, Fraile G, Velásquez M, Correia H, Fonseca G, Marín M, Marcano E, Sánchez Y 2002 Studies on the photostability and phototoxicity of aloe-emodin, emodin and rhein *Die Pharmazie* **57(6)** 399-404
[2] Cárdenas C, Quesada A R and Medina M A 2006 Evaluation of the anti-angiogenic effect of aloe-emodin *Cell. Mol. Life Sci.* **63** 3083-3089
[3] Wang C, Zhenzhou J, Yao J et al. 2008 Participation of cathepsin B in emodin-induced apoptosis in HK-2 Cells *Toxicology Letters* **181** 196-204
[4] Wang C, Wu Xudong, Chen M, Duan W et al. 2007 Emodin induces apoptosis through caspase 3-dependent pathway in HK-2 cells *Toxicology* **231** 120-128
[5] Brown S B, Brown E A and Walker I 2004 The present and future role of photodynamic therapy in cancer treatment. *Lancet Oncol.* **5** 495-508
[6] Teng Z et al. 2007 Cellular absorption of anthraquinones emodin and chrysophanol in human intestinal caco-2 cells *Biosci. Biotechnol. Biochem.* **71 (7)** 1636-1643
[7] http://bilrc.caltech.edu/files/filecabinet/folder5/RamanHandbook.pdf
[8] Kneipp K et al. 1999 Ultrasensitive chemical analysis by Raman *Chem. Rev* **99** 2957-2975
[9] Kneipp K et al. 1998 Extremely large Enhancement Factors in Surface-Enhanced Raman Scattering for Molecules on Colloidal Gold Clusters *Applied spectroscopy* **52 (12)** 1493-1497
[10] Hering K et al. 2007 SERS: a versatile tool in chemical and biochemical diagnostics *Springer-Verlag Anal Bioanal Chem (2008)* **390** 113-124
[11] Tian Z Q, Yang Z L, Ren B and Wu D Y 2006 SERS from transition metals and excited by ultraviolet light *Topics in Applied Physics* **103** 125-146
[12] Lee P C and Meisel D 1982 Adsorption and Surface-enhanced Raman of dyes on silver and gold sols *J. Phys. Chem.* **86** 3391-3395
[13] http://www.fcsxpert.com/classroom/theory/what-is-confocal-volume.html
[14] Rao S, Bálint S, Lovhaugen P, Kreuzer M, Petrov D 2009 Measurement of mechanical forces acting on optically trapped dielectric spheres induced by surface-enhanced raman scattering *Physical Rev. Lett.* **102** 087401
[15] Mikhailyuk I K and Razzhivin A P 2003 Background Subtraction in Experimental Data Arrays Illustrated by the Example of Raman Spectra and Fluorescent Gel Electrophoresis Patterns *Instruments and Experimental Techniques* **46, 6** 765-769
[16] Sánchez-Cortés S, Jancura D, Miskovsky P, Bertoluzza A 1996 Near infrared surface-enhanced Raman spectroscopic study of antiretroviraly drugs hypericin and emodin in aqueous silver colloids *Elsevier Spectrochimica* Acta Part A **53** 769-779
[17] http://www.tiem.utk.edu/bioed/webmodules/diffusion.htm
[18] http://hyperphysics.phy-astr.gsu.edu/hbase/biology/celmem.html
[19] Ferraro J R, Nakamoto K and Brown C W 2003 *Introductory Raman Spectroscopy* (California: Academic Press)
[20] Campion A and Kambhampati 1998 Surface-enhanced Raman scattering *Chemical Society Rev.* **27** 241-250
[21] http://nte-serveur.univ-lyon1.fr/spectroscopie/raman/H1TUTO~1.htm
[22] Petrov D 2007 Raman spectroscopy of optically trapped particles *Journal of applied A: pure and applied optics* **9** S119-S156